Journal of Applied Sciences 10 (18): 2019-2026, 2010
ISSN 1812-5654


# Heat Transfer Characteristics of Intake Port for Spark Ignition Engine: A Comparative Study

[1,2]M.M. Rahman, [1]K.I. Hamada, [1]M.M. Noor, [1]K. Kadirgama, [3]M.A. Maleque and [1]R.A. Bakar
[1]Department of Mechanical Engineering, University Malaysia Pahang, 26600 Pekan, Kuantan, Pahang, Malaysia
[2]Automotive Excellence Center, University Malaysia Pahang, 26600 Pekan, Kuantan, Pahang, Malaysia
[3]Department of Manufacturing and Material, Engineering Faculty of Engineering, International Islamic University Malaysia, Gombak, Selangor, Malaysia

**Abstract:** This study presents a comparative study of heat transfer characteristics in intake port for spark ignition engine using hydrogen and methane as a fuel. The fuels are led to the different behavior of physical processes during the engine cycle. One-dimensional gas dynamics was used to describe the flow and heat transfer in the components of the engine model. The engine model has been simulated with variable engine speed and equivalence ratio ($\phi$). Engine speed has been varied from 2000 to 5000 rpm with increment of 1000 rpm, while equivalence ratio has been changed from stoichiometric to lean limit. The baseline engine model has been verified with existing previous published results. The obtained results are shown that the engine speed has the same effect on the heat transfer coefficient for hydrogen and methane fuel; while equivalence ratio is effect on heat transfer coefficient in case of hydrogen fuel only. Rate of increase in heat transfer coefficient comparison with stoichiometric case for hydrogen fuel are: 4% for ($\phi$ = 0.6) and 8% for ($\phi$ = 0.2). While negligible effect was found in case of methane fuel with change of equivalence ratio. But methane is given greater values about 11% for all engine speed values compare with hydrogen fuel under stoichiometric condition. The blockage phenomenon affects the heat transfer process dominantly in case of hydrogen fuel; however the forced convection was influencing the heat transfer process for hydrogen and methane cases.

**Key words:** Engine speed, equivalence ratio, hydrogen fuel, intake port, heat transfer rate coefficient, methane

## INTRODUCTION

Fossil fuels represent the major energy sources in the world. Unfortunately, a lot of harms accompanied the use of these sources. Among the gaseous fossil fuels, natural gas, which consists of about 90% methane, is gaining acceptance because of its low emission levels and alternative energy source concerns (Arici, 1993). One of the important alternative fuels is hydrogen. Hydrogen is a very efficient and clean fuel. Its combustion produces no greenhouse gases, no ozone layer depleting chemicals and little or no acid rain ingredients and pollution. Hydrogen, produced from the renewable energy (solar, wind, biomass, tidal etc.) sources, would result in a permanent energy system which would never have to be changed (Kahraman *et al*., 2007; Rahman *et al*., 2009a, b). Hydrogen internal combustion engine ($H_2$ICE) is a technology available today and economically viable in the near-term. This technology demonstrated efficiencies in excess of today's gasoline engines and operate relatively cleanly (Nox is the only emission pollutant) (Boretti *et al*., 2007). Increases efficiencies, high power density and reduce emissions are the main objectives for internal combustion engine development (White *et al*., 2006). One of the major parameter that effective in the improvement of performance and emission regulation in the ICE is the amount of heat loss during the combustion process. Therefore, the accurate model describes the heat transfer phenomena for $H_2$ICE, which gives important information that required to improve the simulation of engine performance.

The heat is convected from the intake port wall to the mixture charge. Heat transfer mainly caused by forced convection, which is controlled by turbulent charge movement and the temperature gradient of the mixture charge to the wall. Whilst surveying the correlations for use in model of quasi-steady heat transfer in the piping system of internal combustion engine. Schubert *et al.* (2005) noticed that the correlations are mostly based on the similarity theory developed by Nuβelt:

**Corresponding Author:** M.M. Rahman, Automotive Excellence Center, Faculty of Mechanical Engineering, Universiti Malaysia Pahang, 26600 Pekan, Kuantan, Pahang, Malaysia Tel: 6094242246 Fax: 6094242202

$$\alpha = \frac{d}{k_f}.C.Re^m \quad (1)$$

where, $\alpha$, d and $k_f$ are heat transfer coefficient, cylinder diameter and fluid thermal conductivity, respectively.

The classical, steady correlations in the form of $Nu = CRe^m$ or $Nu = CRe^mPr^n$ are widely used for estimating the convective heat transfer coefficient in the intake manifolds of engines (Dittus and Boelter, 1930; Bauer *et al*., 1998; Depcik and Assanis, 2002; Shayler *et al*., 1996) because of a correlation type and the easy-to-use as well as unsteady heat transfer model is not available. The constants C, m and n are adjusted to match the experimental data to account for unsteady heat transfer enhancements, surface deposits and surface roughness. Steady state correlations constants are listed in Table 1.

The amount of heat transfer is converted from the intake port wall to mixture charge calculates according to the Newton's law of cooling as Eq. 2:

$$Q = \alpha A \ (T_g - T_w) \quad (2)$$

where, Q, A, $T_g$ and $T_w$ are amount of heat transfer, heat transfer area, gas temperature and wall temperature, respectively.

In addition, frequencies based on valve events as well as pipe lengths, drastically alter the flow patterns and change the heat transfer relationship (Depcik and Assanis, 2002). Besides, type of the working gas another parameter will give a significant effect on the heat transfer process. These correlations provide reasonable agreement with experimental data in fully-developed steady pipe flows and acceptable agreement with time-resolved experimental data in unsteady flows and slow velocity variation under the quasi-steady assumption. However, these correlations can produce large errors in both phase and magnitude (Zeng and Assanis, 2004) for highly unsteady flows with rapid velocity variation. Experimental results published by different researchers show that the unsteady flow effect in the engine intake manifold enhances heat transfer by 50 to 100% over the prediction of the steady pipe flow correlation presented by Dittus and Boelter (1930). At different engine speed and load conditions, the unsteadiness of the flow condition is different. Therefore, the constants (C and m) are usually optimized only for one operating condition of a given engine and hence compromised for other conditions.

Table 1: Steady state correlations constants

| Reference of previous study | C | m | n |
|---|---|---|---|
| Dittus and Boelter (1930) | 0.0230 | 0.800 | 0.4 |
| Bauer *et al.* (1998) for straight manifold | 0.0620 | 0.730 | 0.0 |
| Bauer *et al.* (1998) for curved manifold | 0.1400 | 0.660 | 0.0 |
| Depcik and Assanis (2002) | 0.0694 | 0.750 | 0.0 |
| Shayler *et al.* (1996) | 0.1350 | 0.713 | 0.0 |

The physical properties of hydrogen fuel differ significantly from those fossil fuels (Li and Karim, 2006; Verhelst and Sierens, 2001). This provides the impetus for the authors to verify the heat transfer process inside intake port for hydrogen fueled engine and specify the differences with methane. Thus, the heat transfer process will be taken into account for the present study to demonstrate the ability of the heat transfer correlations which basically found for intake port with hydrocarbons fueled engine to represent heat transfer process inside intake port with hydrogen fueled engine as well as features detection of heat transfer phenomenon for the intake port with the new alternative fuel.

## MATERIALS AND METHODS

This study was conducted at Automotive Excellence Centre, Faculty of Mechanical Engineering, Universiti Malaysia Pahang, Kuantan. The duration of the project is April 2009 to August 2010.

**Engine model:** A single cylinder four stroke spark ignition port injection with two valves (one inlet and one exhaust) model was developed utilizing GT-Power software. The injection of fuel was located in the midway of the intake port. The computational model of single cylinder hydrogen fueled engine is shown in Fig. 1. The schematic diagram for the model is demonstrated in Fig. 2. The engine specifications are shown in Table 1. The specific engine characteristics are used to make the model A is shown in Table 2. It is important to indicate that the intake and exhaust ports of the engine cylinder are modeled geometrically with pipes. The characteristics of the intake port of engine are shown in Table 3. The intake and

Table 2: Engine specifications for model (A)

| Parameters | Value | Unit |
|---|---|---|
| Bore | 100.0 | mm |
| Stroke | 100.0 | mm |
| Connecting rod length | 220.0 | mm |
| Compression ratio | 9.5 | - |
| Inlet valve open | 9.0 | CA(BTDC) |
| Exhaust valve open | 55.0 | CA(BBDC) |
| Inlet valve close | 84.0 | CA(ABDC) |
| Exhaust valve close | 38.0 | CA(ATDC) |
| No. of cylinder | 1.0 | - |

Table 3: Intake port characteristics

| Intake port parameter (unit) | Value |
|---|---|
| Diameter at inlet end (mm) | 40 |
| Diameter at outlet end (mm) | 40 |
| Length (mm) | 80 |
| Surface roughness (mm) | 0 |
| Wall temperature (K) | 340 |

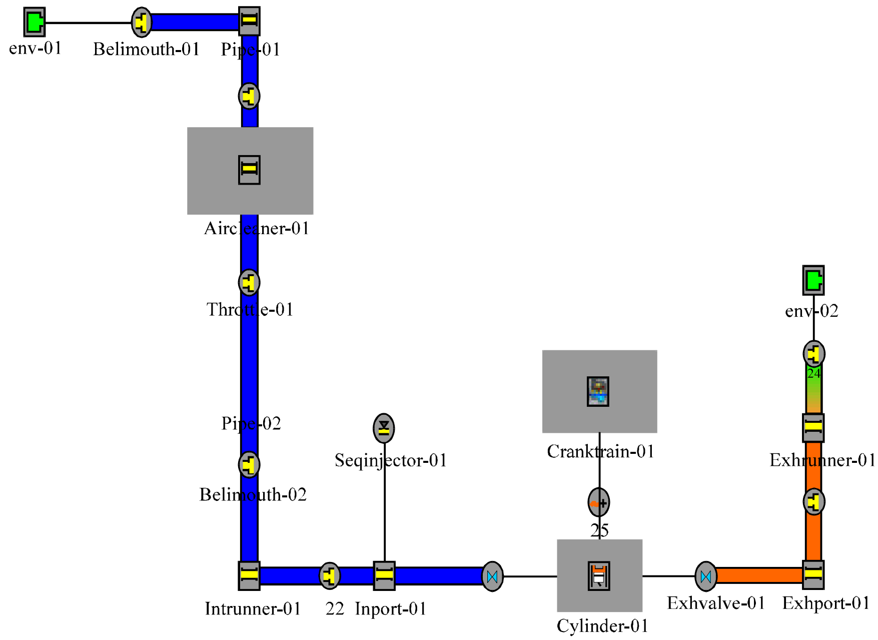


Fig. 1: Model of single cylinder four stroke, port injection engine

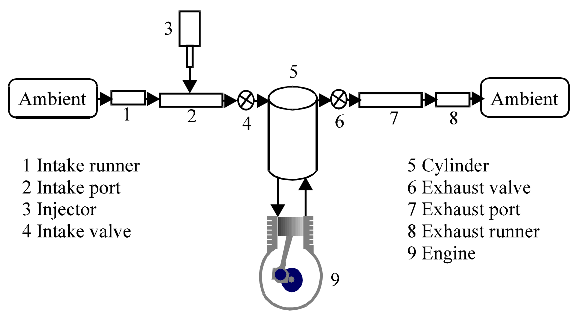


Fig. 2: Schematic diagram for the model

exhaust ports of the engine cylinder are modeled geometrically with pipes and the air enters through a bell-mouth orifice to the pipe. The discharge coefficients of the bell-mouth orifice were set to 1 to ensure the smooth transition. The diameter and length of bell-mouth orifice pipe are 0.07 and 0.1 m, respectively and it is connected to intake air cleaner with 0.16 m of diameter and 0.25 m of length. A log style manifold was developed from a series of pipes and flow-splits. The total volume of each flow-split was 256 cm$^3$. The flow-splits compose from an intake and two discharges. The intake draws air from the preceding flow-split. One discharge supplies air to adjacent intake runner and other supplies air to the next flow-split. The last discharge pipe was closed with a cup. The flow-splits are connected with each other through pipes with 0.09 m diameter and 0.92 m length. Intake port wall temperature value was assumed according to previous investigation results (Bauer, 1997). The junctions between the flow-splits and the intake runners were modeled with bell-mouth orifice. The intake runners were linked to the intake ports with 0.04 m diameter and 0.08 m length. The temperature of the piston is higher than the cylinder head and cylinder block wall temperature. Heat transfer multiplier is used to take into account for bends, additional surface area and turbulence caused by the valve and stem. The pressure losses are included in the discharge coefficients calculated for the valves and no additional pressure losses were used because of wall roughness (pressure losses have been estimated using dependency on Reynolds number only). The exhaust runners were modeled as rounded pipes with 0.03 m inlet diameter and 800 bending angle for runners 1-4 and 40° bending angle of runners 2 and 3. Runners 1-4 and runners 2 and 3 are connected before enter in a flow-split with 169.646 cm$^3$ volume. Conservation of momentum is solved in 3-dimentional flow-splits even though the flow based on a one-dimensional version of the Navier-Stokes equation. Finally a pipe with 0.06 m diameter and 0.15 m length connects the last flow-split to the environment. Exhaust walls temperature was calculated using a model embodied in each pipe and flow-split. The air mass flow rate in intake port was used for fuel flow rate based on the imposed equivalence ratio ($\phi$). The specific values of input parameters including the equivalence ratio and engine speed were specified in the model. The boundary condition of the intake air was defined first in the entrance of the engine. This object describes end environment boundary conditions of pressure, temperature and composition. The air enters through this object to the pipes. This object describes an orifice placed between any two flow components and its parts represent the plane connecting two flow components. The orifice diameter is set equal to the smaller of the adjacent component diameter on the either side of the orifice. While the orifice forward and reverse discharge coefficients are automatically calculated using the geometry of the mating flow components and orifice diameter, assuming that all transitions are sharp-edged. The hydrogen and methane have been used to represent as a fuel in current study for revealing the difference between of these fuels in term of heat transfer characteristics inside intake port.

**Model governing equations:** One dimensional gas dynamics model is used for representation of flow and heat transfer in the components of the engine model. Engine performance can be studied by analyzing the mass, momentum and energy flows between individual engine components and the heat and work transfers within each component. Simulation of 1-D flow involves the solution of the conservation equations including the mass, momentum and energy in the direction of the mean flow as Eq. 3-5, respectively:

$$\frac{dm}{dt} = \sum_{boundaries} m_{flux} \tag{3}$$

$$\frac{d(m_{flux})}{dt} = \frac{dp.A + \sum_{boundaries}(m_{flux}.u) - 4.C_f.\frac{\rho.u^2.A.dx}{2D}}{dx} - \frac{C_{pl}.(\frac{1}{2}\rho.u^2).A}{dx} \tag{4}$$

$$\frac{d(m_{flux}.e)}{dt} = p\frac{dV}{dt} + \sum_{boundaries} m_{flux}.H - \alpha.A(T_g - T_w) \tag{5}$$

where A, e,V and H are the cross sectional area, specific internal energy, element volume and enthalpy.

All properties for the charge have been computed by solving the above governing equations simultaneously based on explicit technique.

To complete the simulation model other additional formulas beside of the main governing equations are used for calculations of the pressure loss coefficient, heat transfer and friction coefficient. The pressure loss coefficient ($C_{pl}$) is defined by Eq. 6:

$$C_{pl} = \frac{p_1 - p_2}{\frac{1}{2}\rho u_1^2} \tag{6}$$

where, $p_1$ and $p_2$ are the inlet and outlet pressure, respectively, $\rho$ the density and $u_1$ the inlet velocity. The heat transfer from the internal fluids to the pipe and flow split walls is dependent on the heat transfer coefficient, the predicted fluid temperature and the internal wall temperature. The heat transfer coefficient is defined as Eq. 4:

$$\alpha = \frac{1}{2}C_f\rho U_{eff}C_p Pr^{-\frac{2}{3}} \tag{7}$$

where, $U_{eff}$, $C_f$, $C_p$ and Pr are the effective velocity outside boundary layer, friction coefficient, specific heat and Prandtl number, respectively. The effective velocity at any axial location inside intake port was considered as the root-mean-square value of the instantaneous velocity.The friction coefficient for smooth walls can be expressed as Eq. 8:

$$\begin{aligned} C_f &= \frac{16}{Re_D} \qquad Re_D < 2000;\ Re_D = \frac{vD}{\upsilon} \\ C_f &= \frac{0.08}{Re_D^{0.25}} \qquad Re_D > 4000 \end{aligned} \tag{8}$$

where, $Re_D$ and D are Reynolds number, pipe diameter and roughness height, respectively.

The Prandtl number can be expresses as Eq. 9:

$$Pr = \frac{\upsilon}{\lambda} \tag{9}$$

where, $\upsilon$ and $\lambda$ are the kinematic viscosity and thermal diffusivity, respectively. The amount of heat rate which is transferred from the inlet charge inside the intake port to its walls calculates according to the formula of Newton's law of cooling (Eq. 2).

## RESULTS

Steady state gas flow and heat transfer simulations for the in-cylinder of four stroke port injection spark ignition engine model fueled. The hydrogen and methane is considered as a fuel with two operation parameters namely equivalence ratio ($\phi$) and engine speed. The equivalence ratio was varied from stoichiometric limit ($\phi$ = 1.0) to a very lean limit ($\phi$ = 0.2). The equivalence ratio was change with interval of 0.2. The engine speed varied from 2000 rpm to 5000 rpm with interval of 1000 rpm. The heat transfer coefficient was used as an indicator for heat transfer characteristics to reveal the difference between hydrogen and methane fuels.

Table 4: Specifications of the engines models

| Engine parameter | Lee *et al.* (1995) | Present model B | Unit |
|---|---|---|---|
| Bore | 85 | 85.0 | mm |
| Stroke | 86 | 86.0 | mm |
| TDC clearance height | NA* | 3.0 | mm |
| Piston pin offset | NA | 1.0 | mm |
| Connecting rod length | NA | 150.0 | mm |
| Compression ratio | 8.5 | 8.5 | - |
| Inlet valve open | 16 | 16.0 | $^0$CA(BTDC) |
| Exhaust valve open | 52 | 52.0 | $^0$CA(BBDC) |
| Inlet valve close | 54 | 54.0 | $^0$CA(ABDC) |
| Exhaust valve close | 12 | 12.0 | $^0$CA(ATDC) |

*NA: Not available

**Model validation:** In the present study were approved by adopting experimental results from two previous works. General assessment for the model performance is dedicated in the first validation while the second validation is devoted for revealing the extent and reliability of model results compared with previous existing correlation for intake port heat transfer. The experimental results obtained from Lee *et al.* (1995) were used for purpose of first validation in this study. Engine specifications of Lee *et al.* (1995) and present single cylinder port injection engine model (B) are shown in Table 4. The same engine model which described in Fig. 1 was used for the purpose of first validation (taking into account the difference in the engines dimensions). Engine speed and equivalence ratio were fixed at 1500 rpm and ($\phi$ = 0.5), respectively in this comparison to be coincident with Lee *et al.* (1995) results.

The in-cylinder pressure traces for the baseline model (B) and experimental previous published results (Lee *et al.*, 1995) are shown in Fig. 3. It can be seen that in-cylinder pressure trace are very good match for compression stoke and acceptable trends for expansion strokes while large deviation was obtained for combustion period due to the delay in the combustion for experimental as in claim's of Lee *et al.* (1995), beside the difference between the some engine configuration conditions that is not mentioned by Lee *et al.* (1995). However, considerable coincident between the present model (B) and experimental results can be recognized in spite of the mentioned model differences. To demonstrate the effectiveness of the adopted model for the present study model (A), direct comparison with model (B) in term of in-cylinder pressure traces was done as shown in Fig. 4. The difference between two models is due to the difference in dimensions and compression ratio between of two models. Correlation which introduced by Depcik and Assanis (2002) is used for the purpose of model verification specifically for the intake port heat transfer in present study. This correlation was proposed by using a least square curve-fit of all available experimental data to get a general relationship which

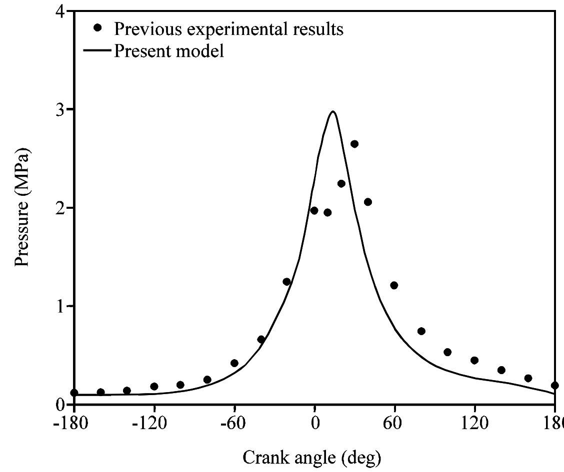


Fig. 3: Comparison between published experimental results (Lee *et al.*, 1995) and present single cylinder port injection engine model (B) based on in-cylinder pressure traces

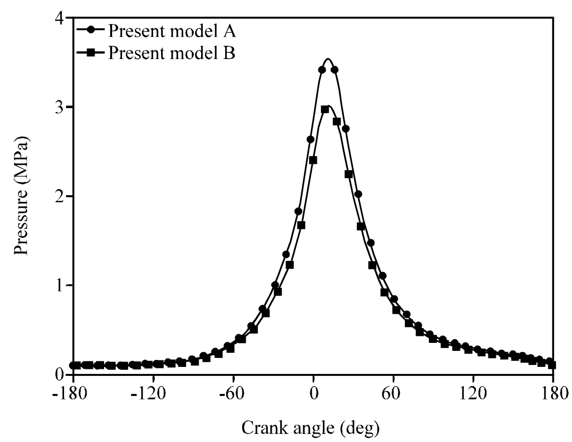


Fig. 4: Comparison between models (A and B) based on in-cylinder pressure traces

describe a dimensionless heat transfer coefficient Nu with Reynolds number expressed as Eq. 10:

$$Nu = 0.0694Re^{0.75};\ 1500 < Re < 40000 \qquad (10)$$

Direct comparison between the acquired results from the engine model (A) and the getting results from empirical correlation for hydrogen and methane fuel is represented. Variation of heat transfer coefficient with engine speed for hydrogen and methane with stoichiometric mixture is revealed in Fig. 5. It's clear that the correlation performance for describing of methane fuel give a good agreement with engine model results, where the deviation is 11% within correlation limit and 16%

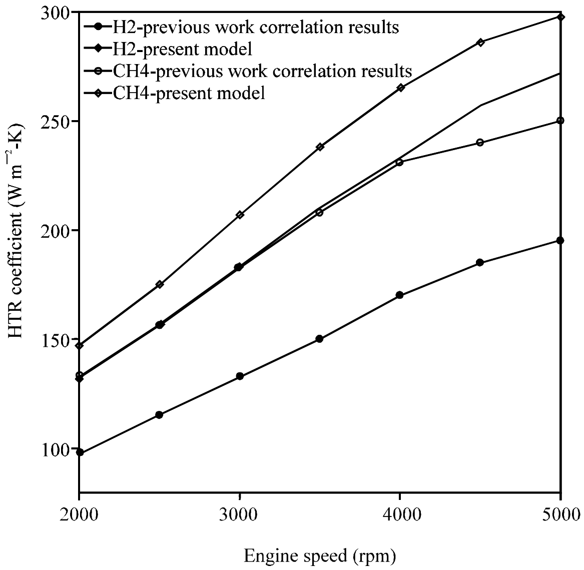


Fig. 5: Comparison between previous study (Depcik and Assanis, 2002) and present model A for heat transfer coefficient

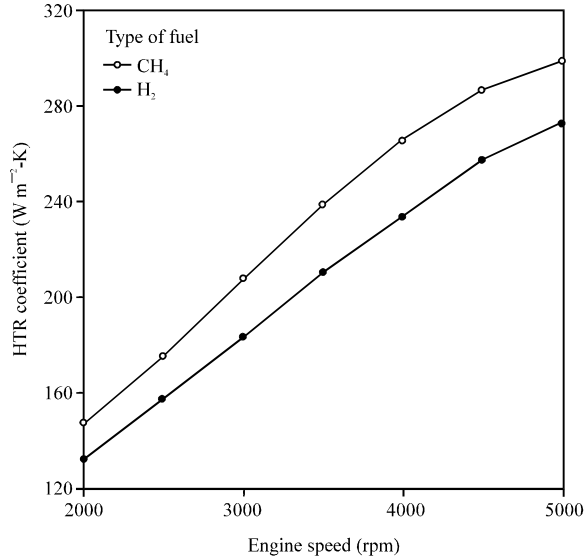


Fig. 6: Variation of heat transfer coefficient with engine speed for equivalence ratio $\phi$ = 1.0

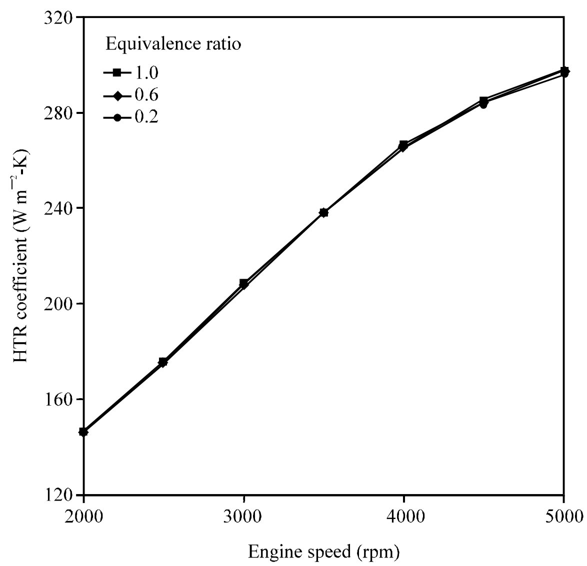


Fig. 7: Variation of heat transfer coefficient on for methane fuel against speed and equivalence ratio

outside this limit, if taking into consideration both of the deviation and limitation for the original correlation compared with the original experimental results which used for fitting. Where, correlation have an r-value (deviation factor) of 0.846 and applicable with range Reynolds number (1500<Re<40000) (Depcik and Assanis, 2002) which correspond to engine speed values equal to (1500<RPM<4000) for methane and (1500<RPM<4500) for hydrogen. The same trends achieved for the hydrogen fueled engine model. Through this comparison can be determined the extent and reliability model adopted in the present study. While, the correlation results was under prediction for the performance of model (A) in case of hydrogen fuel with deviation equal to 28%. This result is expected because the correlation was derived mainly for hydrocarbon fuels.

**Heat transfer coefficient for intake port:** Comparison between hydrogen and methane in term of heat transfer coefficient and their behavior with changes of engine speed and equivalence ratio ($\phi$) represents as indicator used to reveal the characteristics of steady state heat transfer inside the intake port for port injection $H_2$ICE. Direct comparison between hydrogen and methane in term the variation of heat transfer coefficient with engine speed is described in Fig. 6. The heat transfer coefficient is increasing as engine speed increase for methane and hydrogen fuels with keeping the highest values for methane fuel.

Effect of equivalence ratio ($\phi$) on heat transfer coefficient with variation of engine speed is shown in Fig. 7 and 8 for methane and hydrogen, respectively. The difference between methane and hydrogen behavior is very clear in term of equivalence ratio ($\phi$). In case of methane there are no effect (or negligible) for equivalence ratio ($\phi$) on the values and behavior of heat transfer coefficient. As a result, it is expected that there will be no any impact for this variable on the overall process of heat

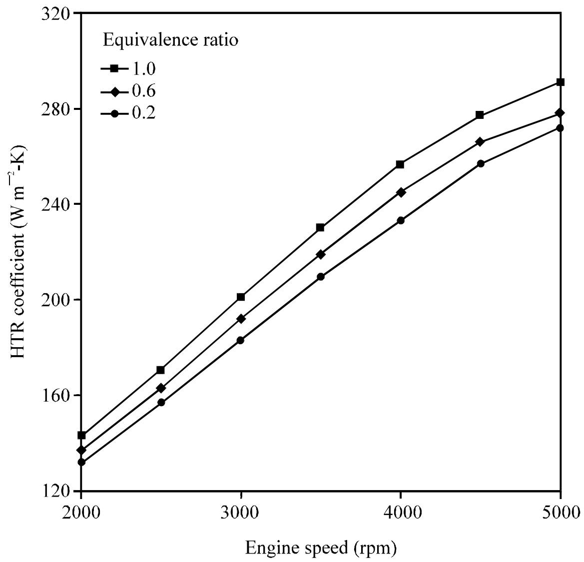


Fig. 8: Variation of heat transfer coefficient for hydrogen fuel with speed and equivalence ratio

transfer. On the contrary, it can be seen the impact of this factor in case of hydrogen. It decreases the equivalence ratio (ϕ) values heat transfer increase due to disappear of the blockage phenomenon.

## DISCUSSION

The effects of engine speed and equivalence ratio on heat transfer coefficient are illuminated in case of hydrogen and methane fuels in the previous section. The behavior of heat transfer coefficient is found to be governed by the blockage and forced convection effects. Forced convection effects are related to engine speed variation while the blockage effects related to equivalence ratio variation. It can be seen that increases of heat transfer coefficient with engine speed increases due to increasing the driving force for the heat transfer process (forced convection) for hydrogen. The similar trends were observed for methane fuel however methane is given greater values about 11% for engine speed compare with hydrogen fuel. The similarity of heat transfer coefficient behavior with variation of engine speed is expected because there is no relation between engine speed and fuel properties. Density of methane fuel is greater than hydrogen as well as the diffusion coefficient for methane is lesser than hydrogen, hence the blockage effect for hydrogen fuel is greater than methane so that the present of forced convection with methane is more strength due to the high restriction for the charge flow in case of hydrogen fuel. Therefore, the heat transfer effect is more efficient in case methane fuel. The results are coincident with previous results which are acquired by Dittus and Boelter (1930), Bauer *et al*. (1998), Depcik and Assanis (2002) and Shayler *et al*. (1996) with some difference in heat transfer coefficient because of the variation for adjusting constants which are function for experimental conditions.

The variation of equivalence ratio (ϕ) in case of methane fuel has a very minor influence on heat transfer coefficient inside intake port. On the other hand, in case of hydrogen fuel, by decreasing the equivalence ratio (ϕ) lead to enhancement of heat transfer characteristics due to the deterioration for the blockage effect consequently. The flow of gas becomes more fluently that means the effect of the forced convection is more strength. This difference in heat transfer coefficient behavior with change of the equivalence ratio due to the large difference in physical properties in terms of density and diffusivity. Rate of increase in heat transfer coefficient comparison with stoichiometric case for hydrogen fuel are: 4 and 8% for the equivalence ratio of 0.6 and 0.2, respectively.

## CONCLUSION

The present study considers the comparison in heat transfer characteristics inside the intake port for port injection engine fueled with hydrogen and methane, respectively. The foregoing results indicates that heat transfer coefficient in the intake port is changed with variation of engine speed and equivalence ratio due to the dissimilarity of fuels properties. Comparison between hydrogen and methane in term of heat transfer coefficient and their behavior with change of engine speed and equivalence ratio are clarified that hydrogen is more dependable on equivalence ratio, whilst both of them have the same trend with engine speed variation. The blockage effect was affecting the heat transfer process dominantly in case of hydrogen fuel, due to the low density and high diffusion velocity for hydrogen in comparison with methane.


## ACKNOWLEDGMENT

The authors would like to thank Universiti Malaysia Pahang for provides laboratory facilities and financial support under project No. RDU0903093 and Doctoral Scholarship Scheme (GRS 090121).


## REFERENCES


Arici, M.A., 1993. Numerical prediction of mixing process in a methane-fueled engine. Ph.D Thesis, Texas Technological Univ., Lubbock. USA.

Bauer, W.D., 1997. Heat transfer and mixture vaporization in intake systems of spark ignition engines. Ph.D. Thesis, Massachusetts Institute of Technology, USA.. http://hdl.handle.net/1721.1/10421.

Bauer, W.D., J. Wenisch and J.B. Heywood, 1998. Averaged and time-resolved heat transfer of steady and pulsating entry flow in intake manifold of a spark-ignition engine. Int. J. Heat Fluid Flow, 19: 1-9.

Boretti, A.A., M.J. Brear and H.C. Watson, 2007. Experimental and numerical study of a hydrogen fuelled I.C. engine fitted with the hydrogen assisted jet ignition system. Proceedings of the 16th Australasian Fluid Mechanics Conference, Dec. 2-7, Crown Plaza, Gold Coast, Australia, pp: 1142-1147.

Depcik, C. and D. Assanis, 2002. A universal heat transfer correlation for intake and exhaust flows in an spark ignition internal combustion engine. SAE Technical Paper No. 2002-01- 0372. http://www.sae.org/technical/papers/2002-01-0372.

Dittus, P.W. and L.M.K. Boelter, 1930. Heat transfer in automobile radiators of the tubular type. Univ. Calif. Publ. Eng., 2: 443-461.

Kahraman, E., S.C. Ozcanli and B. Ozerdem, 2007. An experimental study on performance and emission characteristics of a hydrogen fueled spark ignition engine. Int. J. Hydrogen Energy, 32: 2066-2072.

Lee, S.J., H.S. Yi and E.S. Kim, 1995. Combustion characteristics of intake port injection type hydrogen fueled engine. Int. J. Hydrogen Energy, 20: 317-322.

Li, H. and G.A. Karim, 2006. Hydrogen fueled spark-ignition engines predictive and experimental performance. J. Eng. Gas Turbines Power, 128: 230-236.

Rahman, M.M., M.K. Mohammed and R.A. Bakar, 2009a. Trends of rotational speed on engine performance for four cylinder direct injection hydrogen fueled engine. Trends Applied Sci. Res., 4: 188-199.

Rahman, M.M., M.K. Mohammed and R.A. Bakar, 2009b. Air fuel ratio on engine performance and instantaneous behavior of crank angle for four cylinder direct injection hydrogen fueled engine. J. Applied Sci., 9: 2877-2886.

Schubert, C., A. Wimmer and F. Chmela, 2005. Advanced heat transfer model for CI engines. SAE Trans., 114: 695-708.

Shayler, P.J., M.J.F. Colechin and A. Scarisbrick, 1996. Heat transfer measurements in the intake port of a spark ignition engine. SAE Trans., 105: 257-267.

Verhelst, S. and R. Sierens, 2001. Aspects concerning the optimisation of a hydrogen fueled engine. Int. J. Hydrogen Energy, 26: 981-985.

White, C.M., R.R. Steeper and A.E. Lutz, 2006. The hydrogen-fueled internal combustion engine: A technical review. Int. J. Hydrogen Energy, 31: 1292-1305.

Zeng, P. and D.N. Assanis, 2004. Unsteady convective heat transfer modeling and application to engine intake manifolds. Proceedings of the ASME International Mechanical Engineering Congress and RD and D Expo, Nov. 13-19, Anaheim, California USA., pp: 1-9.